







Objective Diagnosis of Depression and Autism Spectrum Disorder Based on fMRI Time Series Statistics

Jakub D. Szukdlarek¹^a, Sjjir J. C. Schielen¹^b, Catarina Dinis Fernandes¹^c, Danny Ruijters^{1,2}^d,
Albert P. Aldenkamp^{1,3}^e and Svitlana Zinger¹^f

¹*Department of Electrical Engineering, Eindhoven University of Technology, The Netherlands*

²*Image Guided Therapy, Philips Healthcare, The Netherlands*

³*Department of Behavioral Sciences, Epilepsy Center Kempenhaeghe, The Netherlands*

Keywords: Functional Magnetic Resonance Imaging, Resting-State Networks, ICA, BOLD, Depression, ASD, Statistics.

Abstract: A common challenge in diagnosing neuropsychiatric disorders is the lack of objective biomarkers. Current diagnostic approaches rely on the subjective interpretation of observations instead of measurements of brain activity obtained using functional magnetic resonance imaging (fMRI). We propose a method for the objective diagnosis of depression and autism spectrum disorder (ASD), marking the first known experiment that explores the diagnostic performance of only fMRI time series statistics. We researched the importance of time series statistics based on ICA and BOLD for ASD diagnosis. Besides well-known statistics, we introduce features based on the first-order derivative and the frequency-domain representation of the signals. The performance of these features is assessed using multiple machine-learning algorithms. A test accuracy of 69% is achieved on a depression dataset consisting of 72 subjects (51 depressed, 21 controls). On an autism dataset composed of 49 subjects (24 ASD, 25 controls), a test accuracy of 67% and 74% is achieved for ICA and BOLD-based methods respectively. The best results on the ASD dataset are related to the lateral sensorimotor network and the right ventral anterior region. These results demonstrate the potential of fMRI time series statistics as objective biomarkers for neuropsychiatric disorders.

1 INTRODUCTION

Neuropsychiatric disorders encompass a wide range of mental health conditions characterized by psychiatric symptoms. Notable examples include depression and autism spectrum disorder (ASD). A significant challenge in diagnosing these conditions is the absence of objective biomarkers (Bernas, 2020). This issue can be addressed with functional magnetic resonance imaging (fMRI) (Santana et al., 2022).


fMRI provides repeated volumetric measurements of the brain. The variations on these measurements form the blood-oxygen-level-dependent (BOLD) signal, from which the brain's activity can be inferred (Glover, 2011). This process can also be conducted while the subject is not engaged in any task, known as the resting state. Diagnosing neuropsychi-


atric disorders can progress from analyzing interactions within and between different regions of interest (ROIs) of the brain.


The brain can be structurally divided into ROIs by a parcellation atlas, or a decomposition-based approach like independent component analysis (ICA) (Beckmann and Smith, 2004). ICA decomposes a multivariate signal into additive, independent, non-Gaussian components, which allow the identification of resting-state networks (RSNs) (Smith et al., 2009). RSNs are spatially independent patterns that correspond with known brain functions and each RSN has an associated time series.


In this paper, we refer to the time series resulting from averaging voxel activity over the ROIs of a parcellation atlas as 'BOLD time series' and those obtained via ICA as 'ICA time series'. We explore fMRI time series statistics as biomarkers for depression and ASD. This paper has three main contributions:


- The first study that directly applies ICA time series statistics for the diagnosis of depression and ASD, based on our knowledge.


^a <https://orcid.org/0009-0001-1049-6412>

^b <https://orcid.org/0009-0005-1223-0449>

^c <https://orcid.org/0000-0002-3967-5836>

^d <https://orcid.org/0000-0002-9931-4047>

^e <https://orcid.org/0000-0003-3362-9756>

^f <https://orcid.org/0000-0001-9357-3067>

- The first comparison of ICA and BOLD for objective ASD diagnosis. Benchmarking both methods allows comparison of their performance.
- Our method allows interpretability of the diagnostic results. It enables the identification of brain regions significant in the disorder.

The rest of the paper is organized as follows. We present the related literature in Section 2 and the methodology in Section 3. The results are reported and discussed in Section 4. Finally, conclusions are drawn in Section 5.

2 RELATED WORK

Diagnosing neuropsychiatric disorders with fMRI is often investigated by analyzing ICA or BOLD time series. Features derived from these signals are used as input for a given classifier or for statistical testing.

2.1 Current Diagnostic Approaches

Current approaches are usually based on functional connectivity (FC) (Ingalhalikar et al., 2021) or effective connectivity (EC) (Cîrstian et al., 2023), which are measures of the relationship between the activities of pairs of ROIs. The research by (Cîrstian et al., 2023) used wavelet coherence as a measure of FC and achieved an accuracy of over 80% in differentiating the depressed subjects from healthy controls. (Ingalhalikar et al., 2021) used FC to discriminate ASD and controls on the multisite Autism Brain Imaging Data Exchange (ABIDE) dataset. The researchers achieved an accuracy of 71%, which is similar to other studies that diagnose ASD based on FC (Santana et al., 2022). This shows that FC can be used for diagnosing neuropsychiatric disorders. These approaches, however, involve applying complex mathematical methods to the time series. This makes it unclear whether the information contained only in the signal's statistics is sufficient to obtain similar diagnostic results.

After feature extraction, the next step typically involves using a classifier to diagnose based on potential feature differences. (Cîrstian et al., 2023) used a support vector machine (SVM) and decision tree classifiers, while (Ingalhalikar et al., 2021) applied both a random forest (RF) and an artificial neural network. Besides using classical machine-learning approaches to classification, deep-learning is also used to perform both classification and feature extraction.

In the paper by (Supekar et al., 2022), the researchers proposed a spatiotemporal deep neural network (stDNN) model for ASD diagnostics, where

BOLD time series are used as an input to the stDNN directly. Their model achieved 78% accuracy, 76% precision, and 82% recall on the ABIDE dataset. Other papers report combining multimodal features with deep learning and linear SVM (Sen et al., 2018) or graph signal processing (Brahim and Farrugia, 2020). (Liu et al., 2024) used stacked sparse denoising autoencoders and multilayer perceptrons in an ensemble leading to a diagnostic performance of 75.2% accuracy, 82.9% sensitivity, 69.7% specificity on ABIDE I. This shows a shift from classical methods to deep learning-based approaches. While deep-learning methods provide promising results, they employ a high-dimensional decision space, limiting the interpretability of the results. This leaves room to investigate if a small set of statistical features could help clinical practice by making the diagnostics more explainable.

2.2 Statistics-Based Diagnosis

Relatively few studies focus on time series statistics. (Brahim and Farrugia, 2020) proposed a framework combining features derived from graph signal processing and BOLD time series statistics. Classifying with these features resulted in 60% accuracy, 53% sensitivity, and 69% specificity on the ABIDE dataset. Their study notes that first-order statistical features, such as the standard deviation of fMRI time series, "may be a discriminating feature for the classification of a mental disorder like autism" (Brahim and Farrugia, 2020). Further literature suggests that the power spectral density (PSD) of the ICA time series may be discriminating in the case of ASD (Dekhil et al., 2018) and that statistics of the BOLD time series are correlated with dynamic functional connectivity (Zheng et al., 2023). This suggests that the time series statistics should be explored as feasible biomarkers for diagnosing neuropsychiatric disorders.

2.3 ICA and BOLD Time Series

Time series are acquired depending on the parcellation into ROIs, which can be done through ICA or an atlas. Where an atlas divides the brain according to predefined delineations, ICA finds patterns of similarly activating voxels directly on the studied sample. While an atlas and ICA both yield time series representing brain activity, it is unclear how the differences in defining ROIs affect the diagnostics. According to (Moghimi et al., 2022), no optimal brain parcellation atlas exists. This suggests research in which diagnostics based on the BOLD time series are compared to the one based on the ICA time series.

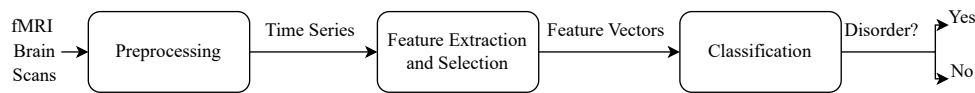


Figure 1: Flowchart for the fMRI time series processing.

Another challenge in diagnostics is the “curse of dimensionality”, which might happen if the number of features used for diagnosis is much higher than the number of included subjects (Berisha et al., 2021). An atlas typically contains more ROIs than ICA, meaning more features for classification. This motivates a comparison between the two.

3 METHODOLOGY

A system for diagnosing neuropsychiatric disorders is proposed. The system can be seen in Figure 1 and consists of fMRI brain scan preprocessing, feature extraction and selection, and binary classification.

3.1 Data Preprocessing

This study utilizes a depression dataset (Bezmaternykh et al., 2022) and the ASD dataset from the Trinity Centre for Health Sciences site, part of the ABIDE dataset (Di Martino et al., 2014). The depression dataset includes 51 depressed subjects (13 males, 38 females, mean age of 33.1 years) and 21 controls (6 males, 15 females, mean age of 33.8 years). The autism dataset consists of 24 subjects with ASD (all males, mean age of 17.3 years) and 25 controls (all males, mean age of 17.1 years).

First, fMRI scans are preprocessed to decrease noise and to normalize the data. Preprocessing is handled in the FMRIB Software Library tool MELODIC 3.0. Steps taken for both datasets involve realignment, slice timing correction, spatial normalization, smoothing, denoising, group ICA and dual regression (Beckmann and Smith, 2004). The ASD dataset is denoised using ICA AROMA (Pruim et al., 2015). For a detailed description of the preprocessing on the depression dataset, see (Cîrstian et al., 2023).

To obtain the BOLD time series, both the AAL3 atlas (Rolls et al., 2020) and the Harvard-Oxford atlas (cort-maxprob-thr25-2mm) (Makris et al., 2006) are used. Voxel time series are averaged over each ROI yielding one time series per ROI. The RSNs were selected using the “goodness-of-fit” (Bernas, 2020), a similarity score between identified ICA components and the Smith atlas (Smith et al., 2009). Independent components were chosen based on the highest obtained score and visually verified.

The resulting RSNs for the depression dataset included: the Primary and Medial Visual Network, Lateral Visual Network, Default Mode Network Anterior, Default Mode Network Posterior, Cerebellum, Sensorimotor Network, Auditory Network, Executive Network, Frontoparietal Right Network, and Frontoparietal Left Network, Lateral Motor Network, and the Dorsal Attention Network (Cîrstian et al., 2023).

For the ASD dataset, the identified RSNs included: the Primary Visual Network, Default Mode Network, Precuneus, Dorsal Attention Network, Salience Network, Auditory Network, Frontoparietal Left Network, Frontoparietal Right Network, Lateral Sensorimotor Network, Occipital Visual Network, Primary Sensorimotor Network and Cerebellum. These RSNs are visualized in Figure 2.

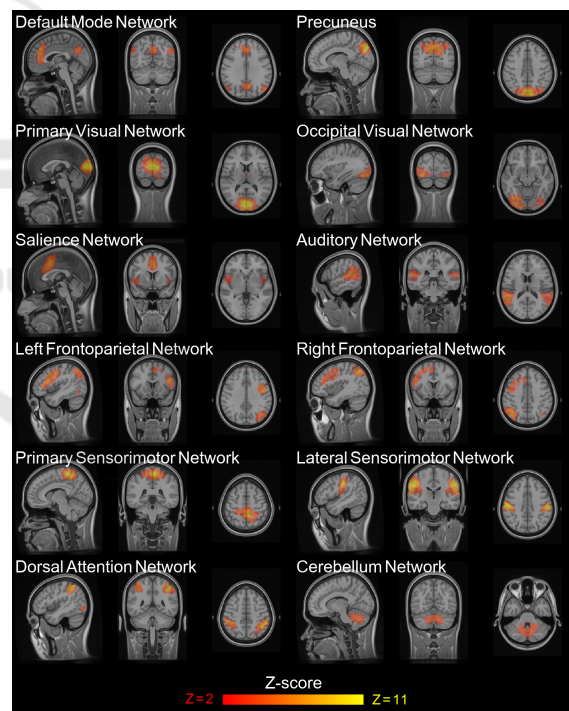


Figure 2: Visual representation of the resting-state networks identified in the ASD dataset. The Z-score represents the level of association between a voxel and a network.

3.2 Feature Extraction and Selection

After preprocessing the data, feature extraction is performed on each of the ROIs’ time series. Features are extracted from the time series (SIG) and its first-order derivative (DER). Subsequently, feature selection is

Table 1: Parameter grids for KNN, SVM, and RF models.

Model	Parameter	Values
K-Nearest Neighbors (KNN)	n_neighbors	[3, 5]
	weights	['uniform']
	metric	['euclidean', 'manhattan']
Support Vector Machine (SVM)	C	[0.1, 0.2, 0.3, 0.4, 0.5, 0.6, 0.7, 0.8, 0.9, 1.0]
	kernel	['linear']
Random Forest (RF)	max_depth	[2, 3]
	min_samples_leaf	[2, 3]
	max_features	['sqrt', 'log2']

applied to the resulting feature vectors (FVs).

Amplitude-based features include the root mean square (RMS), mean value (MV), median (MED), standard deviation (SD), skewness (SKEW), kurtosis (KURT), min. value (MIN), max. value (MAX), range (RAN), and interquartile range (IQR). The RMS and MV are computed according to the equations specified in (Zheng et al., 2023). Then, the SD is calculated as

$$\sigma = \sqrt{\frac{1}{n} \sum_{i=1}^n (x_i - \mu)^2}, \quad (1)$$

where x_i are the indexed time series values, n is the total number of the time points, μ is the MV of the time series and σ represents the SD. To assess a distribution's asymmetry and tail heaviness, SKEW and KURT are computed respectively by

$$\text{SKEW} = \frac{\sum_{i=1}^n (x_i - \mu)^3}{n\sigma^3} \quad (2)$$

and

$$\text{KURT} = \frac{\sum_{i=1}^n (x_i - \mu)^4}{n\sigma^4}. \quad (3)$$

The frequency-based features include the mean frequency (MF), the peak frequency (PF), and the PSD. These features are obtained from the frequency spectrum of the time series. The spectrum is estimated by using Welch's method (Welch, 1967). The PSD was approximated using 26 frequency bins for each RSN. The mean and peak frequency are computed by

$$\text{MF} = \frac{\sum_{f=0}^{f_s/2} f \cdot X(f)}{\sum_{f=0}^{f_s/2} X(f)}, \quad (4)$$

where respectively f_s is the sampling frequency and $X(f)$ is the frequency spectrum of the time series, and

$$\text{PF} = \text{argmax}_f \{X(f)\}. \quad (5)$$

Therefore, thirteen features per ROI are extracted including RMS, MV, MED, SD, SKEW, KURT, MIN, MAX, RAN, IQR, MF, PF, and PSD. These features are aggregated into separate FVs according to

$$\text{FV} = [\text{Feature}_1 \text{ Feature}_2 \text{ Feature}_3 \dots \text{Feature}_N], \quad (6)$$

where FV is the feature vector of a given type, e.g. RMS, MV, etc., Feature_i is a feature of a given type computed for the i -th ROI and N is the total number of ROIs considered in the analysis. These FVs are obtained for both the SIG and DER, resulting in 26 vectors to be investigated as potential biomarkers.

All vectors undergo a z-score normalization and the feature selection process. Two feature selection algorithms are tested separately: Analysis of Variance (ANOVA) and Mutual Information (MI). ANOVA assesses the variance between groups of features to determine their discriminating power, while MI evaluates the dependency between features and the label.

3.3 Classification

The data is split 80/20 for training and testing. To address the class imbalance, the Synthetic Minority Over-sampling Technique (SMOTE) is applied (Chawla et al., 2002). Three classifiers are used: K-Nearest Neighbors (KNN), linear SVM, and RF. These classifiers are applied individually and collectively as an ensemble within the Voting Classifier (VC). Hyperparameters are tuned on the training set through five-fold cross-validation with grid search. The parameter grids of each model are listed in Table 1.

The trained classifiers are subsequently tested on the test set. The best-performing RF, KNN, and SVM are incorporated into the VC ensemble. Training and testing are repeated ten times similar to nested cross-validation. The performance metrics include test accuracy (TA), True Positive Rate (TPR), True Negative Rate (TNR), and the Area Under the Receiver Operator Characteristics Curve (AUC).

Classification is performed in stages to determine the optimal combination of signal type (original time series, SIG, or its first-order derivative, DER), feature selection method (ANOVA or MI), classifier, and number of selected features (FS). By systematically varying the mentioned parameters, the study aims to identify the best-performing configuration. This method is applied to both datasets and extended with

Table 2: Highest test results (AUC score) for the depression dataset based on ICA time series statistics (best result in boldface). The tables include: **Feature Vector** - the feature vector used for prediction; **AUC** - Area Under the ROC Curve; **TA** - Test Accuracy; **TPR** - True Positive Rate (Sensitivity); **TNR** - True Negative Rate (Specificity); **Features Selected** - number of features chosen; **Signal** - type of signal used; **Selection Method** - method for selecting features; **Model** - algorithm achieving the reported performance.

Feature Vector	AUC	TA	TPR	TNR	Features Selected	Signal	Selection Method	Model
RAN	0.67	0.69	0.73	0.60	6	DER	MI	RF
RMS	0.66	0.65	0.65	0.66	9	DER	ANOVA	RF
RAN	0.66	0.66	0.67	0.64	7	DER	MI	KNN
MAX	0.66	0.69	0.75	0.57	4	DER	MI	RF
MAX	0.65	0.69	0.77	0.52	5	DER	MI	RF

Table 3: Highest test results (AUC score) for the autism dataset based on ICA time series statistics (best result in boldface).

Feature Vector	AUC	TA	TPR	TNR	Features Selected	Signal	Selection Method	Model
PF	0.67	0.67	0.56	0.78	1	DER	MI	VC
PF	0.66	0.66	0.60	0.72	1	DER	MI	KNN
MAX	0.65	0.65	0.66	0.64	1	DER	MI	SVM
SKEW	0.65	0.65	0.50	0.80	2	DER	MI	RF
SKEW	0.64	0.64	0.74	0.54	5	SIG	ANOVA	SVM

a comparison between ICA and BOLD on the ASD dataset.

4 RESULTS AND DISCUSSION

This section provides and discusses the numerical results of machine learning experiments. The results are listed in Tables 2, 3, 4, 5. The tables show only the five results leading to the highest AUC score.

4.1 Depression Dataset

The results obtained on the depression dataset are presented in Table 2. As shown, the features RAN, RMS, and MAX (extracted from the ICA time series' derivative) provide predictions with test accuracies ranging from 65% to approximately 70%, along with balanced sensitivity and specificity. The highest results are achieved for features extracted from the ICA time series' derivative, indicating that rates of change are more informative in depression. The best performance is achieved by using MI feature selection, which suggests a nonlinear relationship between features and the label. These results show that features relating to the amplitude of the ICA time series' derivative might carry diagnostic information.

The most selected features in the analysis of the depression dataset include the range of the time series' derivative associated with the cerebellum, primary and medial visual network and, lateral visual network. This is consistent with the literature in link-

ing abnormalities in the cerebellum and visual cortex to depression (Cirstian et al., 2023). This finding demonstrates that statistical methods identify the same abnormal ROIs as more complex methodologies. However, due to the small size of the dataset, this method should be validated with more data in future research.

4.2 Autism Dataset

As shown in Table 3, features selected from the PF, MAX, and SKEW FVs achieve the best performance and balanced metrics. Notably, the best result is obtained using the peak frequency of the lateral sensorimotor network (LSMN) extracted from the ICA time series' derivative. This network was linked to ASD in previous research (Botta et al., 2022). One of the conditions associated with ASD is the lack of reciprocity which is observed, e.g., when autistic individuals struggle to identify the emotions of others. Interestingly, it was observed that a disturbance in the sensorimotor network increases the demands of emotion processing (Davis et al., 2017).

To inspect the differences in peak frequency of the LSMN between ASD and control groups, two box plots are provided in Figure 3. As shown, there are visible differences in the median of both groups while the range of values is similar. A higher peak frequency in the ASD group might indicate faster dynamics in the LSMN and the dominance of high-frequency components in the frequency spectrum of the subjects, which can be viewed as a disturbance in the LSMN in the ASD subjects.

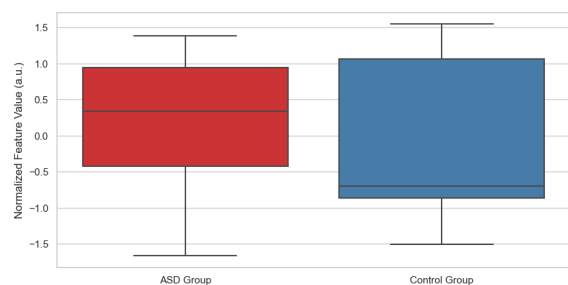


Figure 3: A group comparison of the normalized peak frequency feature of the ICA time series' derivative extracted from the lateral sensorimotor network.

4.3 Comparing ICA and BOLD

The results obtained with the AAL3 atlas are listed in Table 4. Features extracted from the time series achieve higher results more often than the features extracted from its derivative. Comparing the results to Table 3, the features extracted from the derivative signal score higher when ICA is used, while the highest results for the BOLD time series are achieved for features extracted from the original signal. Moreover, predictions based on BOLD time series achieve higher accuracies (over 70%) with balanced sensitivity and specificity. It should be noted that the best results achieved by using both ICA and BOLD time series are obtained when only one feature is considered. In the case of the BOLD time series, features are most often extracted from the right ventral anterior (tVAR).

Notably, tVAR is considered a part of the salience network which was also observed to play a role in ASD (Seeley, 2019). This finding suggests that both ICA and BOLD-based methods identify regions significant in diagnosing ASD, however, they have different focuses. This can be explained by differences in granularity (e.g. 12 RSNs for ICA vs. 166 ROIs in the AAL3 atlas). Therefore, it is unclear which method should be preferred for diagnostics and future research could explore both methods.

To compare the kurtosis between ASD and controls, the mean time series per group are shown in Figure 4. The ASD group has more outliers than the control group which leads to a longer tail of the distribution. As the ASD sample is rather small, this should be verified on a larger dataset such as ABIDE.

To further explore the effect of granularity on the diagnostic performance, the results based on the Harvard-Oxford atlas (consisting of 48 ROIs) are presented in Table 5. As shown, the performance is better than ICA-based predictions but worse than AAL3. An important difference between Table 5 and Table 4 is the fact that the classifiers in Table 5 required a

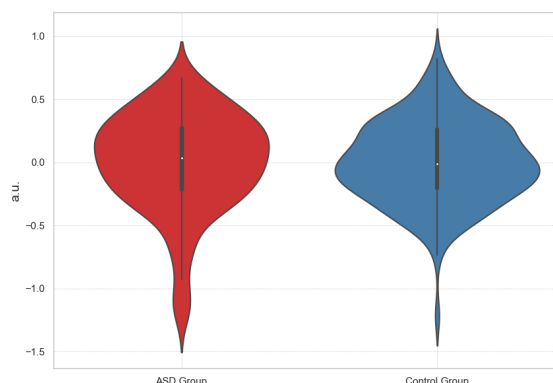


Figure 4: Comparison of the distribution of average time series values between ASD and control groups obtained with the AAL3 atlas. The bigger tail of ASD distribution suggests higher kurtosis for this group.

higher number of features to achieve similar scores. This suggests that when only 48 ROIs are considered, the algorithms struggle to pinpoint the most important region and need more information than with AAL3.

The ROI most often selected for prediction here was the anterior region of the cingulate cortex. Interestingly, it is also a part of the salience network (Seeley, 2019), again showing that the selected features from ICA and BOLD differ. The results show the existence of a few discriminating statistical features. Future work could benefit from exploring a combination of these features, e.g. peak frequency and kurtosis, obtained with different brain parcellations.

5 CONCLUSIONS

The identification of objective biomarkers is essential for objectively diagnosing neuropsychiatric disorders. Currently, such biomarkers are predominantly sought using connectivity-based features. Here, an approach focused on time series statistics was proposed.

This study assessed the feasibility of ICA and BOLD time series statistics as biomarkers for depression and ASD. Results obtained using ICA and BOLD time series were benchmarked against each other on the ASD dataset. The findings indicate that statistical features can carry diagnostic information and relate to RSNs identified in the literature as abnormal. The results also suggest that brain parcellation, i.e. BOLD time series, allows finer brain segmentation and achieves better results than the ICA time series.

The best results on the depression dataset were achieved with the range of the derivative of the cerebellum's ICA time series. For the ASD dataset, the highest results were obtained for the peak frequency of the lateral sensorimotor network (extracted from

Table 4: Highest test results (AUC score) for the autism dataset based on BOLD time series statistics obtained with AAL3 atlas (best result in boldface). The tables include **Feature Vector** - the feature vector used for prediction; **AUC** - Area Under the ROC Curve; **TA** - Test Accuracy; **TPR** - True Positive Rate (Sensitivity); **TNR** - True Negative Rate (Specificity); **Features Selected** - number of features chosen; **Signal** - type of signal used; **Selection Method** - method for selecting features; **Model** - algorithm achieving the reported performance.

Feature Vector	AUC	TA	TPR	TNR	Features Selected	Signal	Selection Method	Model
PF	0.74	0.74	0.78	0.70	1	DER	MI	RF
KURT	0.74	0.74	0.70	0.78	1	SIG	ANOVA	VC
KURT	0.73	0.73	0.68	0.78	1	SIG	ANOVA	KNN
KURT	0.73	0.73	0.72	0.74	1	SIG	ANOVA	RF
KURT	0.71	0.71	0.70	0.82	1	SIG	ANOVA	SVM

Table 5: Highest test results (AUC score) for the autism dataset based on BOLD time series statistics obtained with the Harvard-Oxford atlas (best result in boldface).

Feature Vector	AUC	TA	TPR	TNR	Features Selected	Signal	Selection Method	Model
KURT	0.72	0.72	0.68	0.76	10	DER	MI	VC
KURT	0.71	0.71	0.64	0.78	9	DER	MI	VC
KURT	0.71	0.71	0.54	0.88	10	DER	ANOVA	KNN
KURT	0.70	0.70	0.58	0.82	10	DER	MI	VC
KURT	0.68	0.68	0.60	0.76	8	DER	MI	RF

the derivative of the ICA time series) and of the right ventral anterior region (extracted from the BOLD time series, AAL3). The achieved test accuracies are 69%, 67%, and 74%, respectively.

While the results do not reach the diagnostic performance of deep-learning methods described in the literature (Supekar et al., 2022), (Liu et al., 2024), they are obtained on a small set of statistical features. The identified features are interpretable and show aberrations in networks known to be related to the respective disorders. Besides providing information that enriches knowledge about psychopathology, it is clear what the decision is based on should these features be used in the diagnostic practice. This provides interpretable diagnostic support to the clinician.

This study has three important contributions. First, using the ICA time series to diagnose depression and ASD. Second, comparing ICA and BOLD-based diagnostics. Third, the proposed method identified brain networks and regions that were significant in discriminating between the disorder and control groups. These contributions show that diagnostic approaches based on fMRI time series statistics provide a valuable baseline. If the results of this paper prove reproducible on larger datasets, this paper could mark an advancement toward finding objective biomarkers for depression and ASD.

REFERENCES

- Beckmann, C. F. and Smith, S. M. (2004). Probabilistic independent component analysis for functional magnetic resonance imaging. *IEEE transactions on medical imaging*, 23(2):137–152.
- Berisha, V., Krantsevich, C., Hahn, P. R., Hahn, S., Dasarathy, G., Turaga, P., and Liss, J. (2021). Digital medicine and the curse of dimensionality. *npj Digital Medicine*, 4:153.
- Bernas, A. (2020). *Resting-state fMRI neurodynamics in neuropsychiatric disorders*. PhD thesis, Maastricht University.
- Bezmaternykh, D., Melnikov, M., Savelov, A., and et al. (2022). Resting state with closed eyes for patients with depression and healthy participants. <https://openneuro.org/datasets/ds002748/versions/1.0.0>. Accessed 26 Feb 2024.
- Botta, A., Lagravinese, G., Bove, M., Pelosin, E., Bonassi, G., Avenanti, A., and Avanzino, L. (2022). Sensorimotor inhibition during emotional processing. *Scientific Reports*, 12(1):6998.
- Brahim, A. and Farrugia, N. (2020). Graph fourier transform of fmri temporal signals based on an averaged structural connectome for the classification of neuroimaging. *Artificial Intelligence in Medicine*, 106.
- Chawla, N. V., Bowyer, K. W., Hall, L. O., and Kegelmeyer, W. P. (2002). Smote: Synthetic minority over-sampling technique.
- Cîrstian, R., Pilmeyer, J., Bernas, A., Jansen, J. F., Breeuwer, M., Aldenkamp, A. P., and Zinger, S. (2023). Objective biomarkers of depression: A study

- of granger causality and wavelet coherence in resting-state fmri. *Journal of Neuroimaging*, 33:404–414.
- Davis, J. D., Winkielman, P., and Coulson, S. (2017). Sensorimotor simulation and emotion processing: Impairing facial action increases semantic retrieval demands. *Cognitive, Affective, & Behavioral Neuroscience*, 17(3):652–664.
- Dekhil, O., Hajjdiab, H., Shalaby, A., Ali, M. T., Ayinde, B., Switala, A., Elshamekh, A., Ghazal, M., Keynton, R., Barnes, G., and El-Baz, A. (2018). Using resting state functional mri to build a personalized autism diagnosis system. *PLoS ONE*, 13.
- Di Martino, A., Yan, C.-G., Li, Q., Denio, E., Castellanos, F. X., Alaerts, K., Anderson, J. S., Assaf, M., Bookheimer, S. Y., Dapretto, M., et al. (2014). The Autism Brain Imaging Data Exchange (ABIDE I). Accessed: 14 Mar 2024.
- Glover, G. H. (2011). Overview of functional magnetic resonance imaging. *Neurosurgery Clinics of North America*, 22:133–139.
- Ingalhalikar, M., Shinde, S., Karmarkar, A., Rajan, A., Rangaprakash, D., and Deshpande, G. (2021). Functional connectivity-based prediction of autism on site harmonized abide dataset. *IEEE Transactions on Biomedical Engineering*, 68:3628–3637.
- Liu, X., Hasan, M. R., Gedeon, T., and Hossain, M. Z. (2024). Made-for-asd: A multi-atlas deep ensemble network for diagnosing autism spectrum disorder. *Computers in Biology and Medicine*, 182:109083.
- Makris, N., Goldstein, J. M., Kennedy, D., Hodge, S. M., Caviness, V. S., Faraone, S. V., Tsuang, M. T., and Seidman, L. J. (2006). Decreased volume of left and total anterior insular lobule in schizophrenia. *Schizophrenia Research*, 83(2-3):155–171.
- Moghimi, P., Dang, A. T., Do, Q., Netoff, T. I., Lim, K. O., and Atluri, G. (2022). Evaluation of functional mri-based human brain parcellation: a review. *Journal of Neurophysiology*, 128:197–217.
- Pruim, R. H., Mennes, M., van Rooij, D., Llera, A., Buitelaar, J. K., and Beckmann, C. F. (2015). Ica-aroma: A robust ica-based strategy for removing motion artifacts from fmri data. *NeuroImage*, 112:267–277.
- Rolls, E. T., Huang, C.-C., Lin, C.-P., Feng, J., and Joliot, M. (2020). Automated anatomical labelling atlas 3. *Neuroimage*, 206:116189.
- Santana, C. P., de Carvalho, E. A., Rodrigues, I. D., Bastos, G. S., de Souza, A. D., and de Brito, L. L. (2022). rs-fmri and machine learning for asd diagnosis: a systematic review and meta-analysis. *Scientific Reports*, 12:6030.
- Seeley, W. W. (2019). The salience network: A neural system for perceiving and responding to homeostatic demands. *The Journal of Neuroscience*, 39:9878–9882.
- Sen, B., Borle, N. C., Greiner, R., and Brown, M. R. (2018). A general prediction model for the detection of adhd and autism using structural and functional mri. *PLoS ONE*, 13.
- Smith, S. M., Fox, P. T., Miller, K. L., Glahn, D. C., Fox, P. M., Mackay, C. E., Filippini, N., Watkins, K. E., Toro, R., Laird, A. R., and Beckmann, C. F. (2009). Correspondence of the brain’s functional architecture during activation and rest. *Proceedings of the National Academy of Sciences of the United States of America*, 106:13040–13045.
- Supekar, K., Ryali, S., Yuan, R., Kumar, D., de los Angeles, C., and Menon, V. (2022). Robust, generalizable, and interpretable artificial intelligence-derived brain fingerprints of autism and social communication symptom severity. *Biological Psychiatry*.
- Welch, P. (1967). The use of fast fourier transform for the estimation of power spectra: A method based on time averaging over short, modified periodograms. *IEEE Transactions on Audio and Electroacoustics*, 15:70–73.
- Zheng, Y., Jin, Y., Cao, T., Lin, R., Xu, Y., Cheng, A., Yao, Y., and Xu, L. (2023). Novel linear and nonlinear features for the analysis of dynamic brain functional connectivity. *IEEE Sensors Journal*, 23:13443–13451.